

Short Communication

Facile Fabrication of ZnO-Au Nanocomposite Electrodes for Improved Supercapacitor Properties and Interface Engineering

Xin Zheng^{1,*}, Yihui Sun², Sijia Jin¹, Kang Zhang¹, Yang Li¹, Jiaolong Yan¹, Haiying Qin¹, Hualiang Ni¹

¹ College of Materials & Environmental Engineering, Hangzhou Dianzi University, Hangzhou 310018, PR China

² Zhejiang Hikstor Technology Co. Ltd, Hangzhou 311300, PR China

*E-mail: yencen@hdu.edu.cn

Received: 7 February 2020 / Accepted: 18 March 2020 / Published: 10 June 2020

Interface engineering is an effective approach to modulate device properties. Here, Au nanoparticles were introduced on ZnO nanorod surface to tune the electrode/electrolyte interfacial character. As expected, a capacitance of 281 F/g could be obtained at a current density of 1 mA/cm², which was 53.6% higher than that without Au nanoparticles. Such enhanced capacitance was due to the Schottky junction at the Au and ZnO interface. Specifically, the Schottky heterointerfaces would induce an internal electric field to trap electrons during the charging process so that the additional electrons would be released in the discharge process. In addition, electron transport could be facilitated, and the reaction potential could be lowered because of the Au nanoparticles. The results show the superiority of interface engineering in supercapacitor devices.

Keywords: ZnO@Au Nanorod Arrays; Supercapacitor; Interface Engineering; Schottky Barrier

1. INTRODUCTION

With the explosive development of customer electronics and electric cars, energy storage devices that are eco-friendly and highly efficient have drawn wide attention[1, 2]. Electrochemical supercapacitors are one of the most promising solutions due to demonstrating higher energy densities than Li rechargeable batteries and higher power densities than conventional capacitors[3, 4]. The electrode materials of supercapacitors (SCs) play a decisive role in the device properties. Numerous materials have been found to be suitable as electrode materials in supercapacitors and can be classified into three types: carbonaceous materials [5], conducting organic polymers [6] and metal oxides/hydroxides[7]. Among the metal oxides, zinc oxide (ZnO) nanostructures have become increasingly popular due to their extraordinary physical properties, including a direct band gap (e.g. 3.4 eV), a large exciton binding energy (60 meV), high electron mobility and an ordered morphology, which

exhibits a high surface area[8-10]. Commonly, an electrochemical redox reaction occurs during charge/discharge at the interface between the electrode and electrolyte. Thus, researchers have focused on reducing the transmission path of electrons and enhancing the propagation efficiency. Recently, the hybridization of metal nanoparticles with SC electrode materials as porous host matrices has received universal attention[11-13]. Wei et al. synthesized Au@Co₃O₄ with a hollow polyhedral morphology to achieve a high specific surface area[14]. Pattanauwat et al. designed a graphene/silver structure to improve capacitance[15]. The interfacial engineering of ZnO by inserting a p-n junction or Schottky junction to regulate electronic migration has been achieved in our previous works[16].

In our work, Au nanoparticles decorated on ZnO nanorods (ZnO@Au) were successfully synthesized. The redox peak observed in cyclic voltammetry measurements revealed the character of pseudocapacitors or faradaic capacitors, which have high energy densities. As anticipated, compared with the ZnO sample, the ZnO@Au composite had a better electron transport efficiency and a higher specific capacitance of 281 F/g at a current density of 1 mA/cm², which was an increase of more than 50%. The remarkable improvement in electrochemical performance presented here implied that interface modulation could be a promising route for the promotion of supercapacitor properties.

2. EXPERIMENTAL

2.1. Synthesis of ZnO@Au nanorods

The formation process is schematically shown in Figure 1. Briefly, 0.1 M zinc acetate was spin coated on FTO glass as a seed layer for the highly oriented ZnO nanorods.

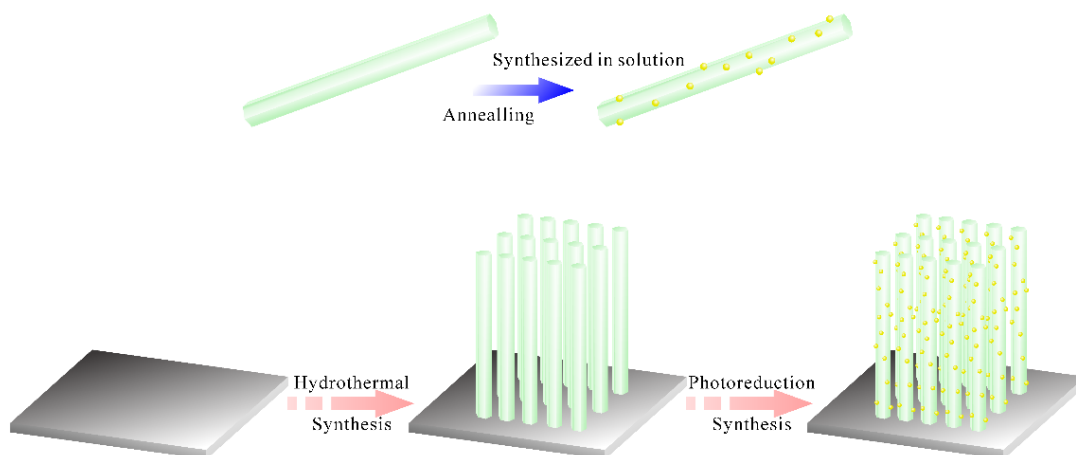


Figure 1. Schematic illustration of the construction of hybrid ZnO@Au nanorod array electrode

Then, the processed FTO was sintered at 350 °C for 30 min. A 100-mL precursor solution was prepared with 0.05 M zinc nitrate hexahydrate and 0.05 M hexamethylenetetramine (HMTA). FTO was placed in the precursor solution at 95 °C for 15 h [17]. Au NPs were synthesized by a photoreduction method and deposited in situ on the ZnO NR arrays by the following procedures. First, 0.05% HAuCl₄

aqueous solution, 1% poly(vinyl alcohol) (PVA) solution, and methanol were mixed together in a proper ratio. The pH of the mixed solution was adjusted to 8 by NaOH. When the Au NPs protected by PVA were negatively charged, the ZnO NR arrays were positively charged. The FTO glass with the ZnO NR arrays was then immersed in the photoreduction solution, and an Ultra Vitalux lamp (OSRAM, 300 W) was used to provide the photoreduction irradiation for 15 min. Next, the ZnO arrays with attached Au nanoparticles were annealed in air at 350 °C for 0.5 h to remove the capped PVA[18].

2.2. Characterization and Measurements

Small pieces of the samples were tailored and pasted onto an aluminium metal table with conductive adhesives for field emission scanning electron microscopy (FESEM, FEI Quanta 3D) observations. The ZnO-Au samples were removed from the FTO glass into an alcohol solution during ultrasonic dispersion. Then, the alcohol solution with the ZnO-Au samples was dropped onto a copper net with a support film for transmission electron microscopy (JEOL, JEM-2010) characterization. Energy dispersive spectroscopy (EDS) measurements were performed to evaluate the structural and elemental properties [17].

2.3. Electrochemical Measurements

Cyclic voltammetry (CV) and galvanostatic charge-discharge measurements were carried out in a conventional three-electrode configuration at room temperature with an electrochemical workstation (SI 1287, Solartron Analytical). The synthesized electrode on the FTO glass acted as a working electrode. A Ag/AgCl electrode and platinum foil served as the reference and counter electrodes, respectively. All electrochemical measurements were carried out in 1.0 mol L⁻¹ KOH electrolyte [17].

3. RESULTS AND DISCUSSION

As the synthesis proceeded, Au particles were deposited on the surface of the ZnO nanorods, and the detailed surface morphologies are shown in Figure 2a. The ZnO nanorods have a diameter of approximately 200 nm and are well aligned on FTO glass. Moreover, the nanorods are hexagonal and have a very clear edge angle, which indicates the high crystallinity of ZnO. The corresponding energy dispersive X-ray spectroscopy (EDS) analysis reveals the presence of Zn, O and Au (as shown in Figure 2a). No signal from other elements exist, indicating the high purity of the obtained electrode materials. The as-prepared products were further characterized by TEM (Figure 2c) to gain a sweeping view of their structure. The TEM observations are in good agreement with the SEM results. The ZnO nanorods are fully and uniformly covered with Au nanoparticles. The HRTEM images of the as-synthesized ZnO@Au composites is presented in (Figure 2d), revealing that a distinct set of the lattice fringes with ZnO (002) plane spacing of 0.26 nm and a Au (111) plane spacing of 0.23 nm.

Thus, the well-organized and successfully prepared electrode materials are conducive for use in supercapacitors.

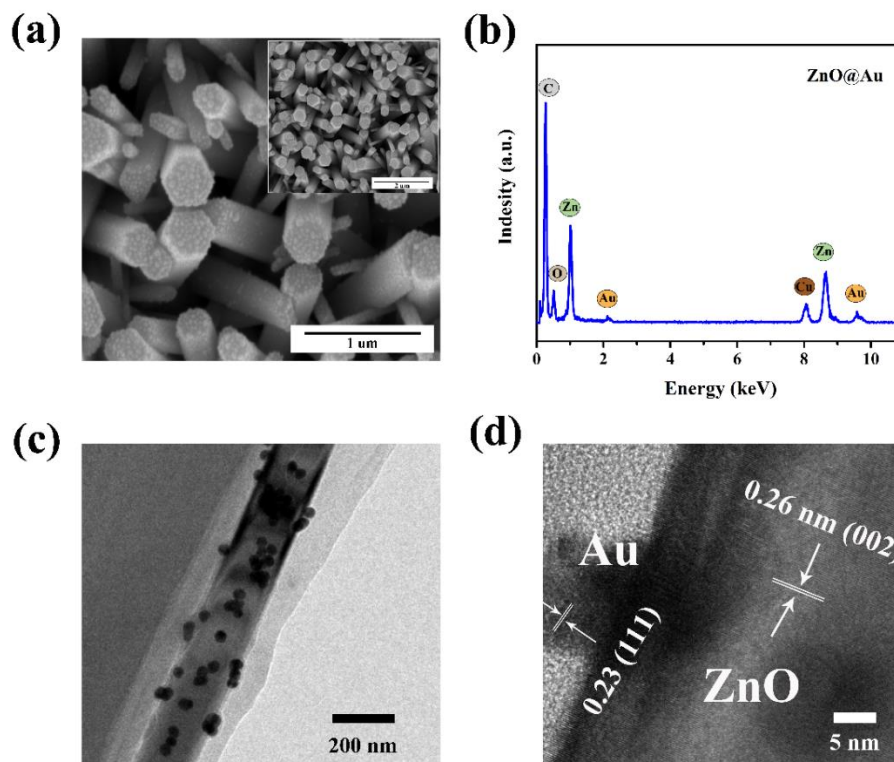


Figure 2. (a) SEM images of the hybrid ZnO@Au nanorod array electrodes. (b) EDX analysis of the the hybrid ZnO@Au nanorod array electrodes. (c) TEM images of the hybrid ZnO@Au nanorod array electrodes. (d) HRTEM images of the hybrid ZnO@Au nanorod array electrodes.

The electrochemical properties of the ZnO nanorod-based 3D electrodes with and without a Au nanoparticle coating were further evaluated by electrochemical measurements in a three-electrode electrochemical cell containing 1 M KOH as the electrolyte. Cyclic voltammetry (CV) measurements were employed within a potential range of 0-0.50 V (vs SCE). The comparison between samples with and without Au NPs are displayed in Figure 3(a) and Figure 3(b), respectively. A redox peak can be clearly observed, and the peak slightly decreases with an increasing scan rate from 5 mV/s to 20 mV/s in both the ZnO sample and ZnO@Au sample. The current density of the ZnO@Au sample is much higher than that of the ZnO sample, and the area is much larger, which indicates the promotion of electron transport and the better electrochemical performance of the Au nanoparticle coating. Additionally, there is an interesting phenomenon in which the position of the redox peak also decreases by 25% from ~0.4 V to ~0.3 V. The decrease in the redox peak position indicates the lowering of the faradaic redox reaction activation energy, which shows a potential advantage in highly efficient electron storage.

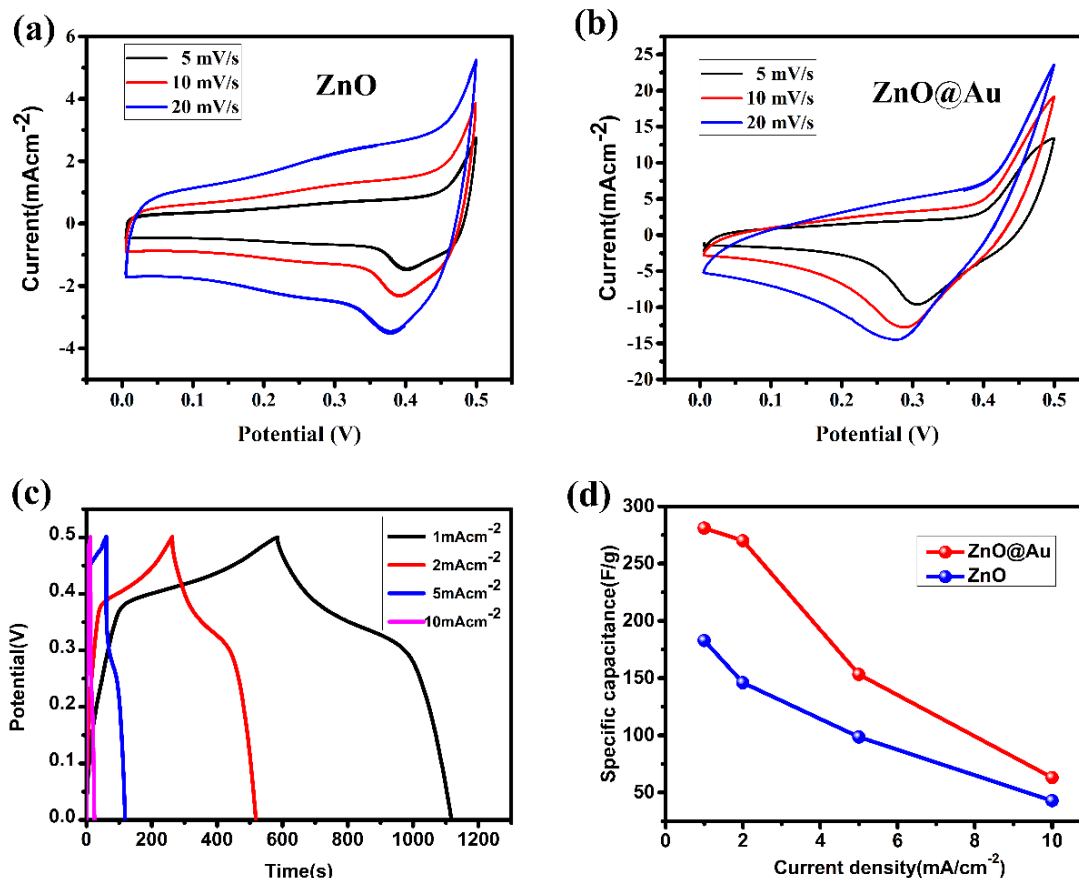


Figure 3. Electrochemical performances of the ZnO nanorods electrodes with & without Au coating measured in 2 M NaOH electrolyte. (a) CV curves of the bare ZnO nanorods electrodes at varying scan rates. (b) CV curves of the hybrid ZnO@Au nanorods electrodes at varying scan rates. (c) Charge-discharge curves of the hybrid ZnO@Au nanorods electrodes at varying current densities. (d) Mass-specific capacitance values of the bare ZnO nanorods and hybrid ZnO@Au nanorods electrodes as a function of current densities.

Galvanostatic charge/discharge curves of the Au nanoparticle-coated ZnO nanorod array were obtained at varying current densities ranging from 1 to 10 A/cm², as shown in Figure 3(c). The nonlinear feature of the discharge curves is in agreement with the CV tests, further confirming the faradaic behaviour of the ZnO@Au 3D structures. The charge/discharge time decreases with increasing current. The average specific capacitance values of the ZnO@Au electrodes with a 3D structure were 281, 270, 153 and 63 F/g at current densities of 1, 2, 5 and 10 mA/cm², respectively; in comparison, the ZnO nanorod electrode exhibited lower specific capacitance values of 183, 146, 99 and 43 F/g, respectively. This difference may come from the enhanced electron transport and high efficiency electron storage, which is revealed in the cyclic voltammetry curves and galvanostatic charge/discharge curves. From the performance comparison with other similar work shown in Table 1 [19], the performance is much better than similar electrodes reported previously.

Table 1. Electrochemical performance comparison with other similar electrodes reported previously

Electrode	Capacitance (Fg ⁻¹)	Current density	Electrolyte	References
ZnO-Au nanoflowers	205	2 Ag ⁻¹	2 M KOH	[19]
ZnO/Ag nanocomposites	189.5	0.5 Ag ⁻¹	1 M H ₂ SO ₄	[20]
ZnO/Au network-like NWA	2 mFcm ⁻²	0.1 mAcm ⁻²	0.2 M Na ₂ SO ₄	[21]
ZnO-Au nanorods	281	1 mAcm ⁻²	1 M KOH	This work

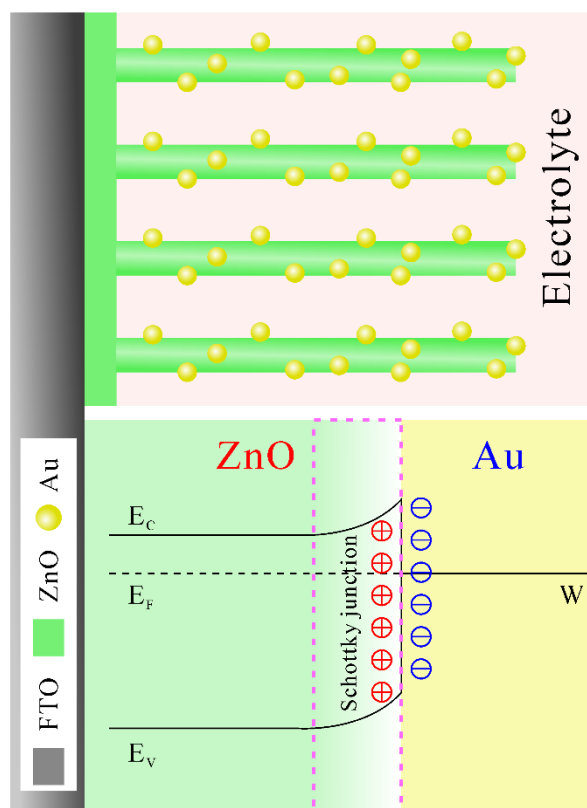


Figure 4. The schematic diagram of Schottky junction in ZnO/Au interface, which help trapping electron during charging and electron transport during discharging.

Heterostructures combining nanomaterials with different band structures can accelerate charge transport and surface reaction kinetics, as mentioned in other works. [22, 23]. The promoted charge

transfer is attributed to the formed internal electric field in the space charge region, such as a P-N junction and Schottky junction. The built-in internal electric field from heterostructures helps electron migration, even without an applied bias, and this technique has been applied in self-powered ultraviolet (UV) detection and other domains. In our work, ZnO is a wide band gap (3.2 eV) n-type semiconductor, whose Fermi level is much higher than the work function of Au. Therefore, a Schottky junction is formed in the Au and ZnO interface after coating Au nanoparticles on the ZnO nanorods, as shown in Figure 4. During the charging process, the electron goes over the Schottky barrier by applying bias. Some of the crossing electrons take part in the redox reaction, while others accumulate in the Au and ZnO interface. The Schottky junction partially acts as the role of capacitor, when applied in a self-powered UV detector, by extending the capacitance of the SC system. During the discharging process, the accumulated electrons will be released and drift. Additionally, the built-in internal electric field will promote electron transport and lower the reaction potential. The fast electron transport channel results in the ZnO@Au sample exhibiting a high current density in the CV tests, as shown in Figure 3(a) and (b). With the help of the Schottky junction from the Au/ZnO interface, the capacitance is enhanced by 84.9% at a current density of 2 mA/cm², which shows the clear advantage of interface engineering for SC devices.

4. CONCLUSION

In this study, Au NP-coated ZnO nanorod-based supercapacitor electrodes were prepared on FTO glass. Compared with a pure ZnO nanorod electrode, the ZnO@Au SC electrodes showed an enhancement of 53.6% in specific capacitance at a current density of 1 mA/cm². The enhancement was due to the Au nanoparticles, which facilitated electron transport and lowered the reaction potential. Additionally, electrons could be trapped by the internal electric field until they filled the potential well during the charging process so the additional electrons would be released in the discharge process. The results provided here offer a new approach to develop high-performance supercapacitors and may be extended to other fields.

ACKNOWLEDGEMENTS

This work was supported by National Nature Science Foundation of China (No. 11847076, 51872069), the Zhejiang Provincial Natural Science Foundation of China (No. LQ19E020005) and Starting Foundation of Hangzhou Dianzi University (No. KYS205618042).

References

1. W. Liu, M.S. Song, B. Kong, Y. Cui, *Advanced Materials*, 29 (2017) 1603436.
2. I. Heng, F.W. Low, C.W. Lai, J.C. Juan, S.K. Tiong, *Journal of Electronic Materials*, 49 (2020) 1777.
3. W. Lai, Y. Wang, Z. Lei, R. Wang, Z. Lin, C.-P. Wong, F. Kang, C. Yang, *Journal of Materials Chemistry A*, 6 (2018) 3933.
4. W. Du, Y.-L. Bai, J. Xu, H. Zhao, L. Zhang, X. Li, J. Zhang, *Journal of Power Sources*, 402 (2018) 281.
5. C. Ramirez-Castro, C. Schütter, S. Passerini, A. Balducci, *Electrochimica Acta*, 206 (2016) 452.

6. Y. Liao, H. Wang, M. Zhu, A. Thomas, *Advanced Materials*, 30 (2018) 1705710.
7. J. Wei, X. Li, H. Xue, J. Shao, R. Zhu, H. Pang, *Advanced Materials Interfaces*, 5 (2018) 1701509.
8. X. Zheng, Y. Sun, X. Yan, X. Sun, G. Zhang, Q. Zhang, Y. Jiang, W. Gao, Y. Zhang, *Journal of Colloid and Interface Science*, 484 (2016) 155.
9. Y. Sun, X. Yan, X. Zheng, Y. Liu, Y. Shen, Y. Zhang, *Nano Research*, 9 (2016) 1116.
10. P. Ghangosar, F. Rigoni, M.G. Kohan, S. You, E.A. Morales, R. Mazzaro, V. Morandi, N. Almqvist, I. Concina, A. Vomiero, *ACS Appl Mater Interfaces*, 11 (2019) 23454.
11. X. Lang, X. Sun, Z. Liu, H. Nan, C. Li, X. Hu, H. Tian, *Materials Letters*, 243 (2019) 34.
12. H. Gao, Y. Cao, Y. Chen, X. Lai, S. Ding, J. Tu, J. Qi, *Journal of Alloys and Compounds*, 732 (2018) 460.
13. W. Hong, J. Wang, Z. Li, S. Yang, *Journal of Materials Chemistry A*, 3 (2015) 2535.
14. F. Wei, W. Liu, X. Zhang, X. Liu, Y. Sui, J. Qi, *Materials Letters*, 255 (2019) 126534.
15. P. Pattanawanuwat, P. Thammasaroj, W. Nuanwat, J. Qin, P. Potiyaraj, *Materials Letters*, 217 (2018) 104-108.
16. X. Zheng, X. Yan, Y. Sun, Z. Bai, G. Zhang, Y. Shen, Q. Liang, Y. Zhang, *ACS Applied Materials & Interfaces*, 7 (2015) 2480.
17. X. Zheng, X. Yan, Y. Sun, Y. Li, M. Li, G. Zhang, Y. Zhang, *Journal of Materials Chemistry A*, 4 (2016) 17981.
18. N. Senthilkumar, M. Ganapathy, A. Arulraj, M. Meena, M. Vimalan, I. Vetha Potheher, *Journal of Alloys and Compounds*, 750 (2018) 171.
19. H. Mahajan, J. Bae, K. Yun, *Journal of Alloys and Compounds*, 758 (2018) 131.
20. K. Rajangam, K.S. Gowri, R.P. Kumar, L.M. Surriya, S.V. Raj, B. Balraj, S. Thangavel, *Materials Research Express*, 6 (2019) 095524.
21. B. Jin, D. Wang, C. Feng, Y. Bi, Z. Jiao, *Catalysis Letters* 146 (2016) 1348.
22. A.M. Navarro-Suárez, K. Maleski, T. Makaryan, J. Yan, B. Anasori, Y. Gogotsi, *Batteries & Supercaps*, 1 (2018) 33.
23. Y. Wang, Y. Lu, K. Chen, S. Cui, W. Chen, L. Mi, *Electrochimica Acta*, 283 (2018) 1087

© 2020 The Authors. Published by ESG (www.electrochemsci.org). This article is an open access article distributed under the terms and conditions of the Creative Commons Attribution license (<http://creativecommons.org/licenses/by/4.0/>).